



Performance of green antiscalants and their mixtures in controlled calcium carbonate precipitation conditions reproducing industrial cooling circuits

Norinda Chhim, Elsi Haddad, Thibaut Neveux, Céline Bouteleux, Sébastien Teychené, Béatrice Biscans

► To cite this version:

Norinda Chhim, Elsi Haddad, Thibaut Neveux, Céline Bouteleux, Sébastien Teychené, et al.. Performance of green antiscalants and their mixtures in controlled calcium carbonate precipitation conditions reproducing industrial cooling circuits. *Water Research*, 2020, 186, pp.116334. <10.1016/j.watres.2020.116334>. <hal-02960036>

HAL Id: hal-02960036

<https://hal.science/hal-02960036v1>

Submitted on 8 Oct 2020

HAL is a multi-disciplinary open access archive for the deposit and dissemination of scientific research documents, whether they are published or not. The documents may come from teaching and research institutions in France or abroad, or from public or private research centers.

L'archive ouverte pluridisciplinaire **HAL**, est destinée au dépôt et à la diffusion de documents scientifiques de niveau recherche, publiés ou non, émanant des établissements d'enseignement et de recherche français ou étrangers, des laboratoires publics ou privés.



HAL Authorization



Open Archive Toulouse Archive Ouverte

OATAO is an open access repository that collects the work of Toulouse researchers and makes it freely available over the web where possible

This is an author's version published in: <http://oatao.univ-toulouse.fr/26768>

Official URL : <https://doi.org/10.1016/j.watres.2020.116334>

To cite this version:

Chhim, Norinda[✉] and Haddad, Elsi and Neveux, Thibaut[✉] and Bouteleux, Céline[✉] and Teychené, Sébastien[✉] and Biscans, Béatrice[✉] *Performance of green antiscalants and their mixtures in controlled calcium carbonate precipitation conditions reproducing industrial cooling circuits.* (2020) Water Research, 186. 116334. ISSN 0043-1354

Any correspondence concerning this service should be sent
to the repository administrator: tech-oatao@listes-diff.inp-toulouse.fr

Performance of green antiscalants and their mixtures in controlled calcium carbonate precipitation conditions reproducing industrial cooling circuits

Norinda Chhim^{a,b}, Elsi Haddad^b, Thibaut Neveux^{a,b}, Céline Bouteleux^{a,b}, Sébastien Teychené^b, Béatrice Biscans^{b,*}

^aEDF Lab Chatou, 6 Quai Watier, 78401 Chatou Cedex, France

^bLaboratoire de Génie Chimique, Université de Toulouse, CNRS, INPT, UPS, 4 Allée Emile Monso CS84234, 31432 Toulouse, France

A B S T R A C T

Cooling circuits in many industrial sectors are faced with daily issues of scaling. One preventive treatment consists in injecting a polymer additive in the circuit to inhibit precipitation of calcium carbonate. Among the used additives, very few are “green” and the efficiency of new candidates are difficult to test directly in industrial conditions. The present study compared performance between two “green” polymer additives, polyaspartic acid (PASP) and polyepoxysuccinic acid (PESA), versus a traditional gold-standard, homopolymer of acrylic acid (HA) in a laboratory scale set-up designed to be representative of an industrial circuit. Results showed that HA and PASP are both inhibitors of calcium carbonate crystal growth. This inhibition resulted from adsorption of polymer additive molecules on the crystal surface, as confirmed by adsorption measurement. Under the same conditions, PESA additive, showed a high rate of calcium ion complexation and a very low inhibition rate. But, PESA was shown to be a nucleation delay. Mixing PESA and PASP can gave nucleation retardation of about 19 h, which approximates the 24 h water residence time in industrial cooling circuits, as well as almost 90% calcium carbonate crystal growth inhibition. This synergy offers promising prospects for preventive scaling treatment.

1. Introduction

Industrial cooling circuits are subject to clogging and deposit of mineral particles such as calcium carbonate (CaCO_3) associated to the suspended matter naturally present in cooling waters. Deposits are localized inside the condenser tubes and on the PVC packing in cooling towers. They can lead to layers of hard scale, increasing heat transfer resistance and thus impairing heat exchange. This is a serious problem in industry, especially in high energy consumption equipment such as thermal and nuclear power plant cooling systems (Neveux et al., 2016; Rahmani et al., 2015), reverse osmosis membrane desalination (Al-Hamzah and Fellows, 2015; Phuntsho et al., 2014), distillation (Al-Rawajfeh, 2008; Ghani and Al-Deffeeri, 2010) and petroleum production (Heming et al., 2015). In electric power plant cooling systems, CaCO_3 precipitation and/or deposition depends on various factors such as circuit operating conditions (temperature range,

concentration factor, water residence time) and circulating water quality (notably, concentrations of calcium and bicarbonate and of suspended matter) (Chhim et al., 2017). Varying hydrodynamic regimes (turbulent in condenser tubes and laminar on the PVC packing of cooling towers) and construction materials (concrete housing, condenser material, PVC packing) also contribute to scale deposition. Technically, deposits impair heat exchange, partially or totally clog tubing and reduce equipment life-expectancy, and financially lead to loss of productivity and increased operating and preventive and curative maintenance costs.

Polymer additives have been widely studied, for their effect on dispersion of suspended matter to reduce clogging and on inhibition of scaling (Hasson et al., 2011; Bu et al., 2016).

Additives commonly used for scale inhibition are polymers containing carboxylic acid groups such as polyacrylic acid (Moulaya et al., 2005; Al-Hamzah et al., 2014; Amjad et al., 2014), polymaleic acid (Shen et al., 2012; Amjad et al., 2014) and polyaspartic acid (Quan et al., 2008; Pramanik et al., 2017), which is a well-known green inhibitor in terms of biodegradability, non-toxicity and non-bioaccumulation (Martinod et al., 2009; Hasson et al., 2011). These polymers have important properties,

* Corresponding author.

E-mail address: beatrice.biscans@toulouse-inp.fr (B. Biscans).

including low concentration effectiveness and high temperature endurance.

Those last years, a lot of efforts have been done to generate green inhibitors. In their review, [Chaussemier et al. \(2015\)](#) focused on some green antiscalants, obtained either by using “natural” organic molecules or extracted from plants. The authors described some positive performance in laboratory tests but underlined that trials of these molecules in pilot plant are limited ([Schweinsberg et al., 2003](#)). However, a study on the inhibition performances of polyaspartic acid on a cooling-water pilot installation by Laborelec company (Belgium) can be found in [Girasa and De Wispelaere \(2004\)](#).

Several works in the literature were focused on polyeoxy-succinic acid (PESA) and polyaspartic acid (PASP) because they are green scale inhibitors given their non-nitrogenous, non-phosphorus, and biodegradable features. Experimental results of [Zhou et al. \(2011\)](#) obtained by static beaker test on inhibition to CaCO_3 , demonstrated that PESA functioned excellent nucleation inhibition to CaCO_3 . The scale inhibition ratio was calculated from the change in cation concentration. Tests were performed at temperature 80°C , solution pH 9.0, and reaction time 10 hr. Above 99.0% of the scale inhibition ratio was obtained when PESA dosage is 30.2 mg/L with 500 and 720 mg/L of Ca^{2+} concentrations.

In another work, [Sun et al. \(2009\)](#) used the reverse osmosis scale inhibitor for static and dynamic study of PESA inhibition at 30°C and pH 7.4. PESA (5, 10, 15 mg/L) was added to the testing water samples. Their results suggest that PESA should be an effective nucleation scale inhibitor that is applicable to reverse osmosis treatment of waters with a wide range of ion compositions. The scale inhibition ratio of PESA is above 90% and at the same water quality is directly proportional to the dosage of PESA, and scale inhibition ratio at the same PESA dosage decreased with the increase of calcium concentration.

[Liu et al. \(2012\)](#) compared the anti-scaling performance of PESA and PASP using the static and rapid controlled precipitation methods (Ca^{2+} : 500 mg/L-1, pH: 9, T: 80°C , t: 8 h). The scale inhibition efficiency, was calculated from the change in cation concentration. During the experiments, the variation in pH and resistivity with time of the water samples was measured. The maximum in the pH-time curves corresponds to the precipitation threshold in the water. In these conditions PESA showed better performance than PASP on nucleation inhibition. Their tests showed that PESA could be very efficient at very low concentration.

More recently [Peronno et al. \(2015\)](#) investigated the inhibition effect of poly(acrylic acid-co-maleic acid) (PAMA) and polyaspartic acid (PASP) on the nucleation/growth process of CaCO_3 in a bulk solution and on a metallic surface using fast controlled precipitation (FCP) method and electrochemical quartz crystal microbalance (EQCM). They showed that these inhibitors were very efficient at low concentration ($4 \text{ mg}\cdot\text{L}^{-1}$) and that they modified the morphology of calcium carbonate crystals.

Moreover, little is known of polymer additive action on scaling under conditions representing river-water quality (pH, supersaturation, suspended matter, etc.) and industrial cooling circuit operation (temperature, residence time, etc.).

Different tests conditions were applied in the previous works cited above for evaluating the inhibition effects of PASP and PESA. It is important to notice that PESA was demonstrated to be a nucleation inhibitor at low concentration, in water initially free of calcium carbonate particles. But considering the previous experimental set-ups, it is difficult to withdraw nucleation and growth kinetics laws separately and to include in these laws process parameters such as supersaturation. Indeed, one of the main issues is of these previous studies is to extrapolate the results to industrial pilot plants.

In our work, seeds of CaCO_3 are introduced in the reactor in order to mimic suspended matter in river water and favor crystal growth in controlled conditions. Inhibition rate is then defined in this work by comparing R_0 and R_a which are respectively calcium carbonate growth rate, in $\text{mol}\cdot\text{m}^{-2}\cdot\text{min}^{-1}$, without and with additive. This enable to use very low quantity of polymers.

In a previous study ([Chhim et al., 2017](#)), the constant composition method, was adapted for calcium carbonate precipitation, in order to replicate experimentally the operating conditions of recirculating cooling water systems, especially with respect to the supersaturation range, presence of suspended matter (such as illite, silica, calcite) and the temperature range encountered. Determination of the thermodynamic driving force (supersaturation) was based on the relevant chemical equilibria, total alkalinity and calculation of the activity coefficients, using PHREEQC software.

In this study, this constant composition method precipitation (constant supersaturation, pH and ionic force) was applied to investigate the influence of polyeoxysuccinic acid (PESA), polyaspartic acid (PASP) and their mixture and to compare the inhibition results to homopolymer of acrylic acid (HA), a classical polymeric additive. So, scaling inhibition performance was investigated through dynamic constant composition precipitation experiments to obtain CaCO_3 growth kinetics in conditions representative of an industrial circuit. The calcium carbonate scale samples were characterized on scanning electron microscopy (SEM) and X-ray diffraction (XRD), and possible mechanisms of inhibition are proposed. These results provide a basis for using new green additives in industrial circulating water systems by synergic treatment of chemicals.

2. Material and methods

2.1. Materials

Commercial calcite powder (99% pure, Merck, reference 1.02066) was used as seeds in all experiments. Measurement of calcite particle size distribution in solution was performed by laser light scattering granulometry showing a mean size of $34.7 \mu\text{m}$ and a specific area of $0.266 \text{ m}^2\cdot\text{g}^{-1}$. Calcium chloride dihydrate (purity 99-105 % ref. 141232.1210) was purchased from Panreac. Anhydrous sodium carbonate (99.95 to 100.05 % purity, ref. 223484) and sodium chloride (ACS reagent, purity $\geq 99.0\%$) were purchased from Sigma-Aldrich.

All the reagents benzethonium chloride, trisodium citrate dehydrate, ethylenediaminetetraacetic acid (with purity $\geq 99\%$) were purchased from Sigma Aldrich.

Green polymer scale inhibitors have been chosen according to the their biodegradability ([Hasson et al., 2011](#); [Harris, 2011](#); [Wilson and Harris, 2011](#)), their lethal concentration and their bioaccumulation properties defined by [Hasson et al \(2011\)](#). They were used as received without any further modification. [Table 1](#) shows the polymers used in this study and their characteristics and suppliers.

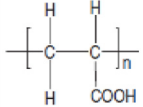
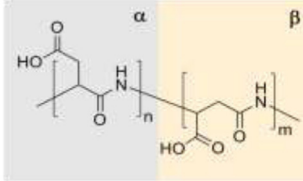
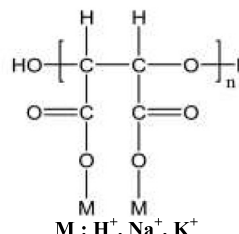
2.2. Constant composition method

[Fig. 1](#) shows the main elements of the constant composition set-up. Precipitation in presence of seeds particles took place in a 1,000 mL agitated double-jacketed reactor. A PTFE cover was designed to minimize the gaseous head space above the solution to prevent ambient CO_2 exchange liable to reduce solution pH.

In each experiment, solution temperature, supersaturation and pH were held constant. A temperature regulator kept working temperatures within the industrial cooling circuit operational range of $25\text{--}45^\circ\text{C}$. A conductivity electrode monitored variation of the ionic force in solution ([Chhim et al., 2017](#)).

Table 1

Characteristics of polymer additives used for calcium carbonate growth inhibition performance tests.

Additive	Molecular weight g.mol ⁻¹	Molecular structure	Initial commercial state	Supplier	Active matter (%)
Homopolymer acrylic (HA) - Reference	2,000		Liquid	Sigma Aldrich	48
Polyaspartic (PASP)	2,000 – 11,000		Solid	Sigma Aldrich	40
Polyepoxysuccinic acid (PESA)	2,000		Solid	Sigma Aldrich	32

The constant composition method relies on the use of two automated burettes, controlled by Tiamo™ 2.5 software (Metrohm), filled with solutions of calcium chloride (reagent 1) and sodium carbonate (reagent 2) corresponding to concentrations of $7.08 \times 10^{-2} \text{ mol.L}^{-1}$ of calcium and carbonate ions (calculated by PHREEC software), respectively and a sensor able to follow reagent consumption due to crystal growth. In the case of calcium carbonate, according to Eq. (1), calcium carbonate precipitation leads to consumption of Ca^{2+} and HCO_3^- ions accompanied by formation of H^+ protons, reducing pH below the threshold value defined initially.



Consequently, a high-precision pH electrode (Unitrode Easy-clean, Metrohm) was used to detect pH variations during CaCO_3 precipitation and to trig reagent injection in order to maintain a constant pH during the precipitation process.

To compensate the reactant consumption due to crystal growth and thus to restore the pH at its initial value, the burettes injected equal volumes of reagents 1 and 2 with a precision of 0.001pH. Injected reagent volume variation over time showed a $\frac{dV}{dt}$ slope on the basis of which the growth rate (R) of calcium carbonate crystals introduced in the reactor, expressed as $\text{mol.m}^{-2}.\text{min}^{-1}$, is given by Eq. (2):

$$R = \frac{dV}{dt} \frac{C_R}{S_T} \quad (2)$$

where $\frac{dV}{dt}$ is the reagent compensation slope in L.min^{-1} , C_R and S_T are respectively the reagent concentration in mol.L^{-1} and the total surface area of the seeds initially introduced in the precipitation reactor (in m^2).

The typical curves obtained during constant composition crystallization experiments are schematically presented in Fig. 2.

In order to study the effect of additives on calcium carbonate precipitation, in conditions that mimic the operating conditions of recirculating cooling water systems, for all the experiments, a set of operating conditions were kept constant and are given in Table 2.

2.3. Calcite crystals characterization

Each synthesized sample was characterized by powder X-ray diffraction (XRD), and scanning electron microscopy (SEM). The powder X-ray diffraction data were collected with a Bruker D8-2 diffractometer equipped with a Bragg–Brentano θ – θ geometry and a copper anode (λ (Cu $K\alpha 1$) = 1.54060 Å and λ (Cu $K\alpha 2$) = 1.54439 Å). The X-ray diffraction patterns were obtained for a range of 2θ angles from 5 to 50° with a step of 0.2°. Scanning electron microscopy (SEM) micrographs were obtained using a SEM-FEG JEOL JSM 7100F microscope. The samples were gold-plated before observation.

2.4. Free Ca^{2+} ion volumetric assay protocol

Free Ca^{2+} ion concentration was assessed by volumetric assay in titrated EDTA (ethylene-diamine tetra-acetic acid) solution at $4.10^{-3} \text{ mol.L}^{-1}$ in presence of 30 μL of colored Patton-Reeder indicator at 1 g.L^{-1} and 1 mL NaOH solution at 2 mol.L^{-1} . To limit solution volume variation in the precipitation reactor due to successive sampling, sample volume was limited to 1 mL and sample number to 3 or 4.

2.5. Measurement of polymer adsorption isotherms

Adsorption experiments were performed in a series of 8 identical hermetically capped bottles. Each bottle was filled with 200mL of supersaturated solution of calcium carbonate, 20mg of calcite seed, and polymer with a concentration ranging from 0.1 to 1.2 mg.L^{-1} . The bottles were immersed in a water thermostatic bath and the temperature was kept constant at 35°C. After 6 days, the solutions were filtered at 0.2 μm , collecting filtrate for assay of residual additive and of calcite seeds for SEM characterization.

Residual additive concentration (C_e) in the solution at 7.6 supersaturation at end of each test was assayed on UV-Visible spectrophotometry using 2 reagents: benzethonium chloride and trisodium citrate dihydrate. The assay principle is based on proportionality between turbidity and additive concentration. Turbidity is

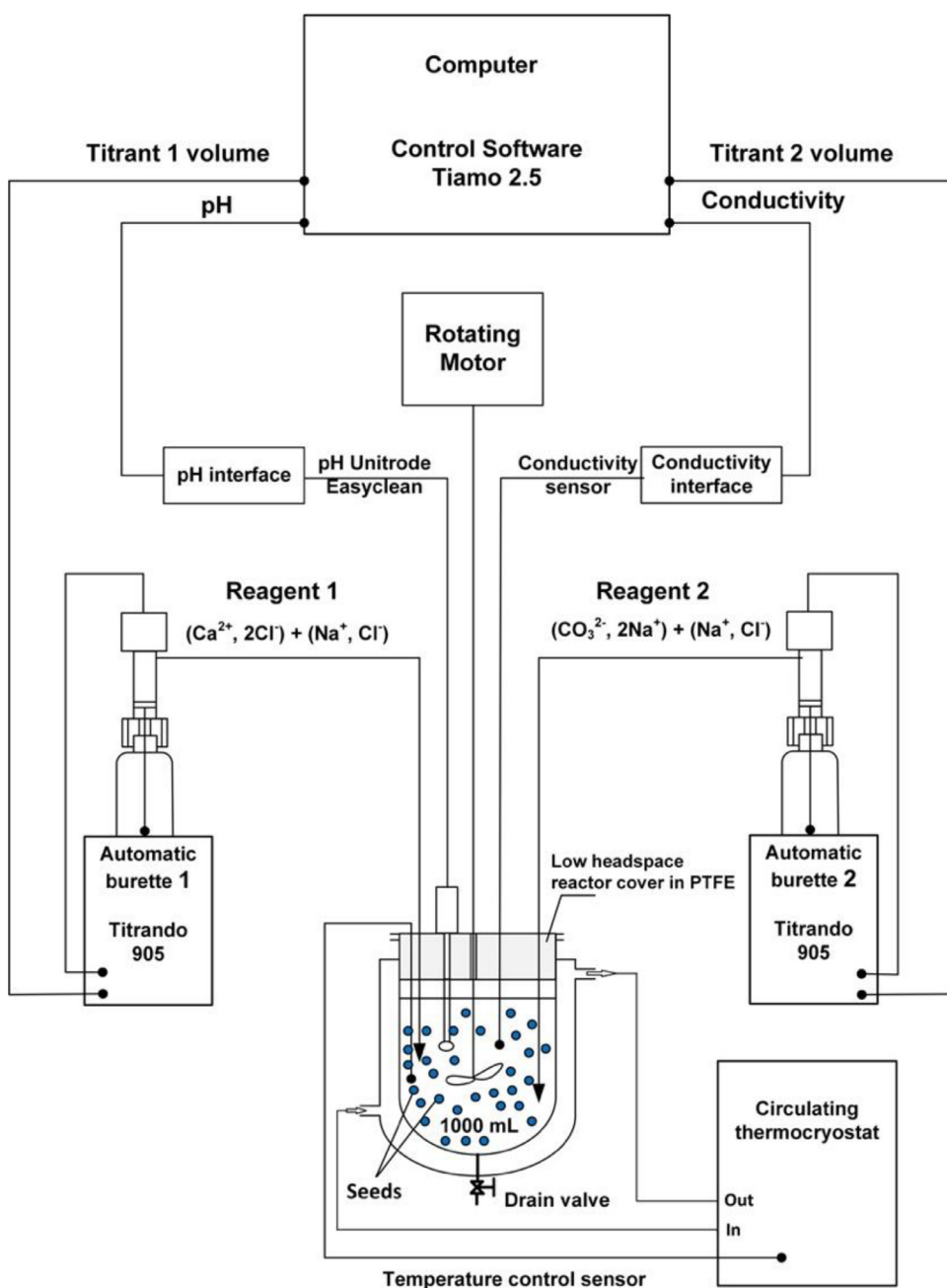


Fig. 1. Laboratory constant composition set-up for kinetic study of calcium carbonate precipitation under conditions representative of industrial cooling circuits.

Table 2

Operating conditions for constant composition precipitation of calcium carbonate experiments.

Parameter	Value
pH	8.5
Ionic Strength ($\text{mol}\cdot\text{L}^{-1}$)	4.24×10^{-2}
Supersaturation $\Omega = \frac{a_{\text{Ca}^{2+}} \cdot a_{\text{CO}_3^{2-}}}{K_s}$	7.6
$a_{\text{Ca}^{2+}}$ and $a_{\text{CO}_3^{2-}}$ activity coefficients	Supersaturation ratio is equivalent to a river-water quality with a mean hardness from 20 to 25°f (200 to 250 $\text{mg CaCO}_3\cdot\text{L}^{-1}$)
Calcite seed concentration ($\text{mg}\cdot\text{L}^{-1}$)	100 The seeds concentration corresponds to values measured in the river during moderate flooding (Idlaflkih et al., 1995)

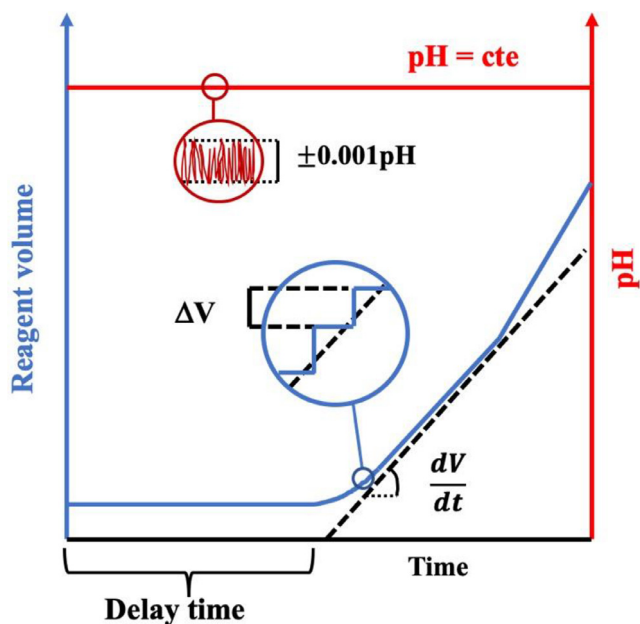


Fig. 2. Typical curve of constant composition crystallization experiment. The step in the volume curve (ΔV) corresponds to the volume resolution of the burette, $\Delta pH=0.001$ corresponds to the resolution of the pH probe. The time between two pH oscillations corresponds to the time resolution of the experiment. The typical blue curve consists of an initial plateau, characteristic of the delay time and of an increase of the volume added corresponding to crystal growth. In some cases, a change of the injected volume is observed and is characteristic of a change in the crystallization mechanism (growth, nucleation or different phase crystallization).

Table 3
Experimental growth rates at constant supersaturation $\Omega = 7.6$ and constant calcite seeds $100 \text{ mg}\cdot\text{L}^{-1}$.

Temperature ($^{\circ}\text{C}$)	25 $^{\circ}\text{C}$	35 $^{\circ}\text{C}$	45 $^{\circ}\text{C}$
Growth rate ($\text{mol}\cdot\text{m}^{-2}\cdot\text{min}^{-1}$)	3.07×10^{-5}	6.07×10^{-5}	11.90×10^{-5}

caused by the reaction between benzethonium chloride and the functional groups of the polymer additive. Trisodium citrate dihydrate is needed to complex the free calcium ions in the sample in order to reduce interference resulting from complexation by polymer additive molecules. All assays were performed on a double-beam Shimadzu 1800 spectrophotometer with 10 cm quartz optical trajectory tanks, with working wavelength set at 306 nm. This tank length reduces the limit of quantification to $0.1 \text{ mg}\cdot\text{L}^{-1}$, enabling assay of low polymer additive concentrations after the adsorption tests (more details on the procedure are given in Appendix).

3. Results

3.1. Crystal growth experiments without additives

To assess the inhibitory effect of the selected additives, reference experiments were performed using the constant composition method for three different temperatures (25 $^{\circ}\text{C}$, 35 $^{\circ}\text{C}$ and 45 $^{\circ}\text{C}$). The chosen temperatures correspond to the operational temperature range of an industrial cooling circuit. Each experiment was repeated at least three times. The evolution of the volume added during the experiment for each experiment are presented in Supplementary Material (Fig. SM1) and calcium carbonate crystal growth rate without additive (R_0), calculated from Eq. (2) are given in Table 3.

Calcium carbonate crystal growth rate (R_0) without additive, based on Eq. (2), increased with temperature (Table 3) in the oper-

ational range of an industrial circuit, suggesting that kinetics under our experimental conditions followed Arrhenius's law relating calcium carbonate growth (R_0) to activation energy (E_a) by Eq. (3):

$$R_0 = k_0 e^{-\frac{E_a}{R_g T}} \quad (3)$$

where R_0 is the growth rate without additive ($\text{mol}\cdot\text{m}^{-2}\cdot\text{min}^{-1}$), k_0 is a pre-exponential constant, E_a is the activation energy ($\text{kJ}\cdot\text{mol}^{-1}$), R_g the universal constant for perfect gas (under normal conditions, $R = 8.314 \text{ J}\cdot\text{mol}^{-1}\cdot\text{K}^{-1}$) and T the absolute temperature (Kelvin).

The activation energy of calcium carbonate growth thus obtained is $53.4 \text{ kJ}\cdot\text{mol}^{-1}$ suggesting that the calcium carbonate precipitation could be surface-controlled or diffusion controlled. This value is in good agreement with the literature involving CaCO_3 precipitation on crystal seeds, where it ranges between 22 and $155 \text{ kJ}\cdot\text{mol}^{-1}$. For example, Parsiegla and Katz (1999) found $45 \pm 4 \text{ kJ}\cdot\text{mol}^{-1}$ and Rodriguez Blanco et al. (2011) found $66 \pm 2 \text{ kJ}\cdot\text{mol}^{-1}$. In the recent work of Cheap-Charpentier et al. (2018) the activation energy ($22 \text{ kJ}\cdot\text{mol}^{-1}$) is related to a scaling process on an immobilized CaCO_3 layer.

At 25 $^{\circ}\text{C}$ and 35 $^{\circ}\text{C}$, Powder X-Ray Diffraction (PXRD) measurements (not shown here) have shown that only calcite crystals were obtained during these experiments. In addition, SEM pictures show well defined calcite crystals with their typical rhombohedral shape, and smooth surface (see Fig. SM2 of Supplementary Material). At 45 $^{\circ}\text{C}$, Powder-XRD characterization have shown that calcite and aragonite were obtained at the end of the experiment. The SEM image presented in Fig. SM2 (supplementary material) shows a typical image of the powder obtained at 45 $^{\circ}\text{C}$. The obtained powder is a mixture of rhombohedral shape crystals as well as needle shape crystals characteristic of the aragonite phase. These results agree with those of Rodriguez Blanco et al. (2011).

3.2. Effect of additive nature on calcium carbonate crystallization

As it was already mentioned in literature (Sun et al., 2009) the scale inhibition ratio of tested additives at the same water quality is directly proportional to their dosage. In the conditions of our experiments, we found that $0.5 \text{ mg}\cdot\text{L}^{-1}$ was the threshold value above which, the inhibition efficiency does not evolve. This additive concentration was then chosen for testing their effect. A first series of experiments was performed at 35 $^{\circ}\text{C}$ to understand the effect of the nature of the additives on the crystallization of calcium carbonate. The results of the constant composition crystal growth experiments obtained for the three tested polymeric additives (HA, PASP and PESA) at a concentration of $0.5 \text{ mg}\cdot\text{L}^{-1}$, are shown in Fig. 3. This figure clearly shows that for PASP and HA, crystal growth starts few minutes after the introduction of seeds and the volume addition rate is much lower than the one obtained without additives. The corresponding slopes and the calculated growth rate are given in Table 4. On the contrary, when PESA is added to the solution, the addition of the reagent starts few hours after the introduction of the seeds in the medium. In addition, when crystallization starts, the reagent addition rate is of the same order of magnitude or higher than the one obtained without additives. Another significant phenomenon, which has been observed only in the experiments performed with PESA, is the increase of pH at the beginning of the experiments, as shown in Fig. 3. To explain this unexpected evolution of pH during the experiment, the amount of free calcium ions in solution was titrated using EDTA. The results show that quickly after the beginning of the experiments, the amount of free Ca^{2+} ions drops from $2.7 \times 10^{-3} \text{ mol}\cdot\text{L}^{-1}$ to $0.65 \times 10^{-3} \text{ mol}\cdot\text{L}^{-1}$. The decrease of free Ca^{2+} induces excess negative charge due to excess HCO_3^- ions in the solution. To ensure solution electroneutrality, CO_2 degassing occurs, accompanied by OH^- ion formation

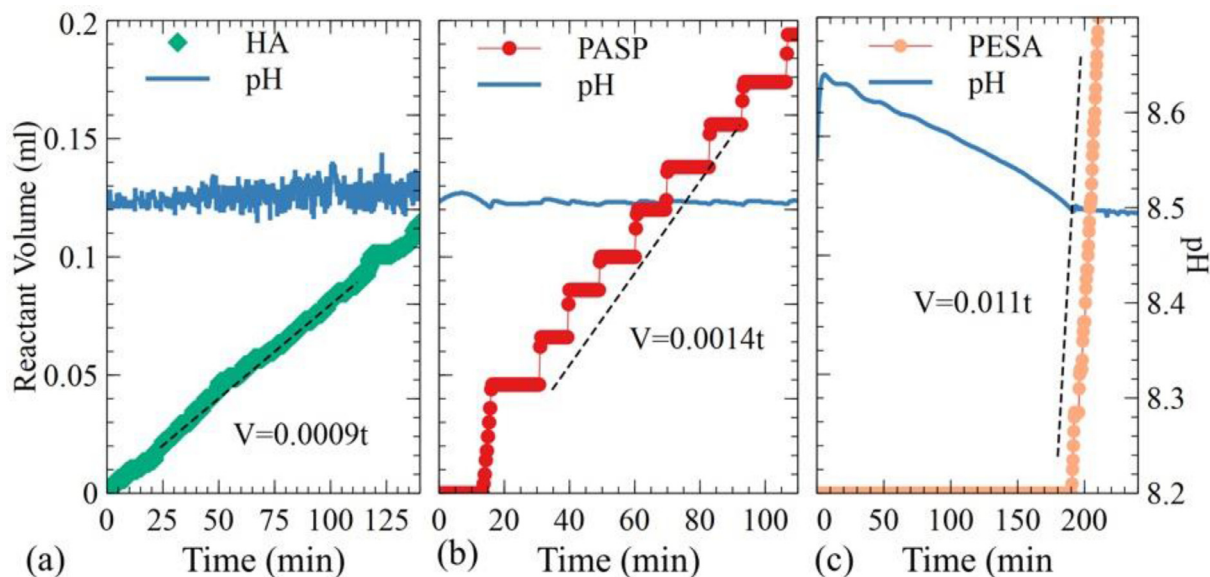


Fig. 3. Temporal evolution of pH and added reagent volume during constant composition experiments performed at $T=35^{\circ}\text{C}$ and $\Omega=7.6$ with (a) HA (b) PASP (c) PESA.

Table 4

Effect of type of polymer additive on calcium carbonate crystal growth inhibition rate and apparent delay time.

Polymer additive	Apparent latency time (min)	R_a ($\text{mol}\cdot\text{m}^{-2}\cdot\text{min}^{-1}$)	Inhibition rate (%)
Homopolymer of acrylic acid (HA)	5.7	4.79×10^{-6}	92.1
Polyaspartic (PASP)	13.3	7.45×10^{-6}	87.7
Polyepoxysuccinic (PESA)	190.3	6.02×10^{-5}	1.0

by a reaction $\text{HCO}_3^- \rightleftharpoons \text{CO}_{2\text{gaseous}} + \text{OH}^-$ (Pesonen et al., 2005). OH^- ion formation in the solution during CO_2 degassing accounts for the rise in pH seen in Fig. 3.

During the pH decrease, formation of CaCO_3 can occur: $\text{Ca}^{2+} + \text{HCO}_3^- \rightleftharpoons \text{CaCO}_3 + \text{H}^+$, forming H^+ ions which neutralize OH^- ions. It is why the delay time before crystal growth is long. After pH reached the setpoint ($\text{pH}=8.5$) and as the quantity of PESA introduced is very low ($0.5\text{mg}\cdot\text{L}^{-1}$) the crystal growth rate obtained is comparable to the one obtained without additive: all the PESA was consumed by complexation. So, PESA turns out to be a nucleation inhibitor with an efficiency of 80%, and hardly inhibits growth (1%).

Table 4 presents results for these three additives at 35°C , 7.6 supersaturation and calcite seeds concentration of $100\text{ mg}\cdot\text{L}^{-1}$, for additive concentration at $0.5\text{ mg}\cdot\text{L}^{-1}$.

Powder characterization shows that when crystallization experiments were performed in presence of HA and PESA, only calcite crystal were obtained as for the crystallization experiments performed without additives.

SEM images performed on crystals obtained in presence of HA (Fig. 4(A)) show that the crystals have the typical rhombohedral shape of calcite. However, compared to the initial seeds, the surface of the crystals seems to be rougher.

In the case of PESA (Fig. 4(C)), the roughness of the crystal surfaces is more pronounced and these surfaces present some vacancies, and the crystals seem to be formed with an assembly of sheets.

When crystallization experiments were performed in presence of PASP, XRPD patterns show that vaterite is preferentially crystallized (see Fig. SM3 in Supplementary Material). In addition, SEM images (Fig. 4 (B)) show that a wide range of crystal shapes are obtained: smooth rhombohedral calcite (probably initial seed crystals), porous spherical particles (with a core-shell structure) and spherulitic crystals (wheat sheaf crystals or type 2 spherulites).

3.3. Effect of temperature on scale inhibition

With $0.5\text{mg}\cdot\text{L}^{-1}$ polymer additives in the original solution, under the same conditions as without additive, calcium carbonate growth inhibition decreases with increasing temperature (Fig. 5) within the operating range for an industrial cooling circuit (25 – 45°C). The inhibition rate is given by Eq. (4):

$$\text{Inhibition rate (\%)} = 100 \frac{R_0 - R_a}{R_0} \quad (4)$$

where R_0 and R_a are respectively the growth rate, in $\text{mol}\cdot\text{m}^{-2}\cdot\text{min}^{-1}$, without and with additive.

HA showed the best inhibition performance (94.8% at 25°C , compared to 87.9% for PASP or 3% for PESA at the same temperature), and likewise at other temperatures.

Activation energy was calculated for the three additives. Activation energy with PASP ($84.3\text{ kJ}\cdot\text{mol}^{-1}$) and HA ($76.8\text{ kJ}\cdot\text{mol}^{-1}$) were similar, and much higher than the one obtained without additives, confirming the inhibitory effect of both polymers on crystal growth. Activation energy with PESA ($54.3\text{ kJ}\cdot\text{mol}^{-1}$) was more or less the same as that found previously for calcite seeds without additive ($53.4\text{ kJ}\cdot\text{mol}^{-1}$), suggesting absence of inhibitory action, in contrast to HA and PASP. However, with PESA, apparent delay time (before reagent burette triggering as start of growth) is longer (around 3 hours). These results suggest that, PESA polymer plays a different role in crystal growth inhibition compared to the two other polymers.

3.4. Effect of polymer additive concentration on crystal growth

When the concentration of PESA in the solution increases from $0.1\text{ mg}\cdot\text{L}^{-1}$ to $1\text{ mg}\cdot\text{L}^{-1}$, the addition rate of reagent is almost not affected and is of the same order of magnitude or higher than the one obtained for the experiments performed without additives. However, as shown in Fig. 6, the apparent delay time of

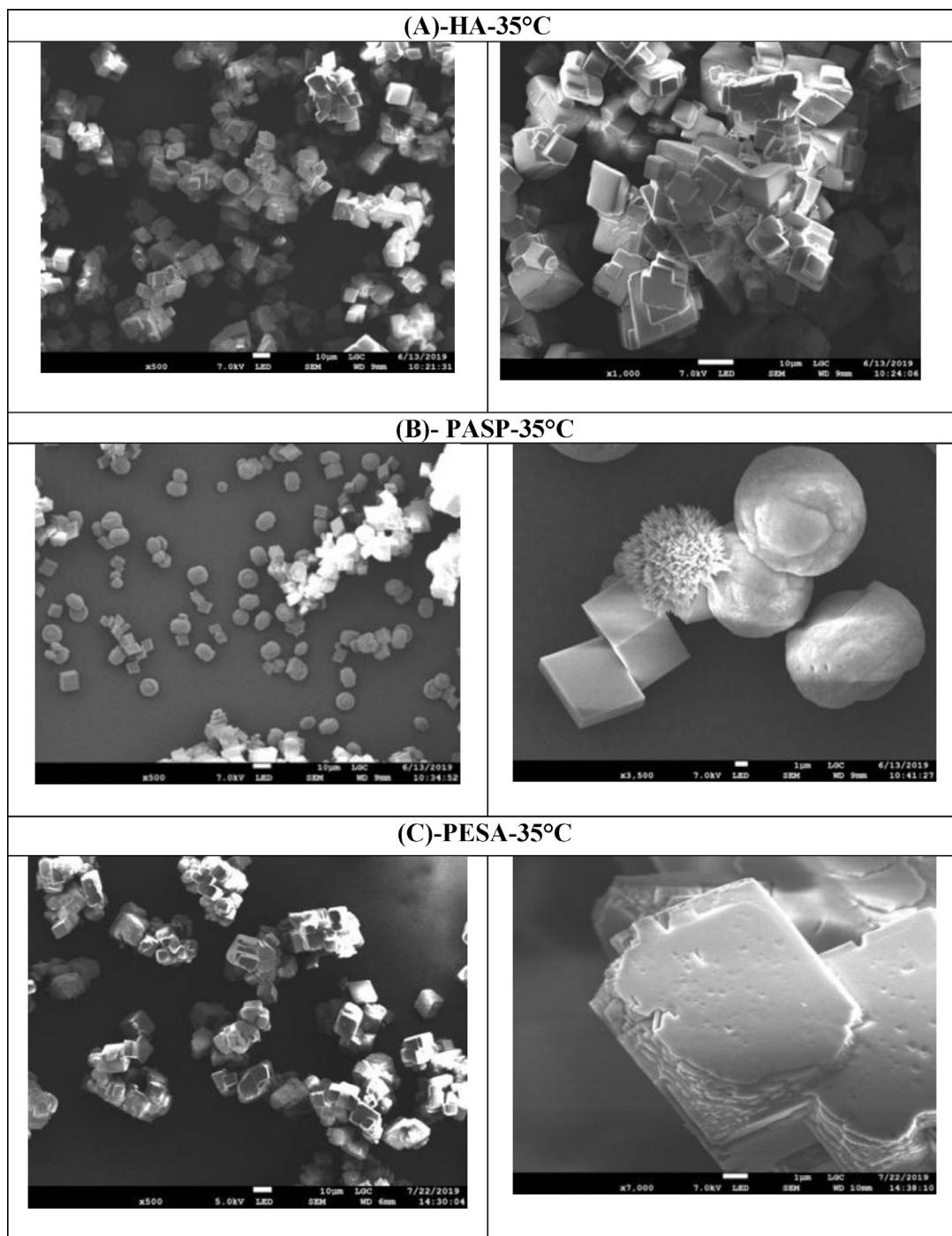


Fig. 4. SEM pictures of grown calcium carbonate seeds with additives: (A) HA; (B) PASP; (C) PESA, at 35°C and 7.6 supersaturation ratio.

crystallization is increased from 63min to 438 min for $C_{PESA}=0.1 \text{ mg}\cdot\text{L}^{-1}$ to $C_{PESA}=1 \text{ mg}\cdot\text{L}^{-1}$. It is worth to note that an increase of pH is observed at the beginning of the experiments for all the concentrations tested.

In the case of HA and PASP, the opposite is observed. The delay time of crystallization is almost not affected by the increase of additive concentration (from 0.1 to 0.5 $\text{mg}\cdot\text{L}^{-1}$) and it ranges from 1 to 10 min. However, when crystallization starts the reagent addition rate, and thus the crystal growth rate, decreases when the additive concentration increases.

By taking the assumption that the crystal growth rate inhibition is due to the polymer adsorption at the surface of the grow-

ing crystal, the polymer additive molecule adsorption characteristics can be derived from these experiments.

The various studies in the literature (Klepetsanis et al., 2002; Kirboga and Oner, 2012; Lioliou et al., 2006) agree on a growth inhibition mechanism involving polymer additive adsorption on the growing crystal surface. We therefore represented the concentration effect by Langmuir's isotherm (Eq. (5)) in the inhibition ratio:

$$\frac{R_0}{R_0 - R_a} = \frac{1}{(1 - b)} + \frac{1}{(1 - b)K_a C_{add}} \quad (5)$$

where R_0 and R_a are the crystal growth rate respectively without and with polymer additive, in $\text{mol}\cdot\text{m}^{-2}\cdot\text{min}^{-1}$; $(1 - b)$ is the

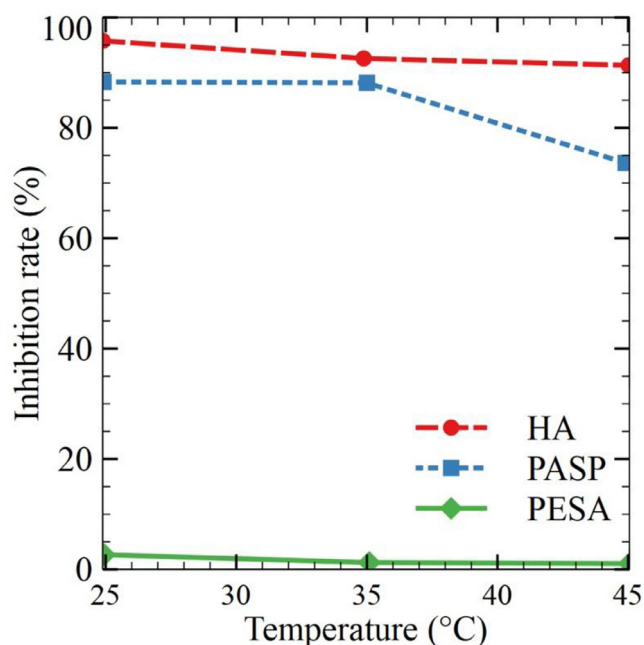


Fig. 5. Evolution of calcium carbonate growth inhibition rate according to temperature for HA, PASP and PESA additives: $\Omega = 7.6$, $C_{\text{additive}} = 0.5 \text{ mg}\cdot\text{L}^{-1}$, calcite seeds $C_{\text{seeds}} = 100 \text{ mg}\cdot\text{L}^{-1}$.

additive efficacy factor; K_a is the adsorption affinity constant for the additive, in $\text{L}\cdot\text{mol}^{-1}$; and C_{add} is the additive concentration, in $\text{mol}\cdot\text{L}^{-1}$.

The additive efficacy factor $(1 - b)$ and adsorption affinity constant (K_a) can be derived experimentally by $\frac{R_0}{R_0 - R_a} = f(\frac{1}{C_{\text{add}}})$. Fig. 7 shows the experimental representation of the inhibition ratio for HA and PASP.

The adsorption constants obtained are reported in Table 5.

In order to test this hypothesis, adsorption experiments of HA and PASP additives on the surface of calcite crystals were performed (the details of the experimental procedure and the data treatments are given in Appendix). The linearized plot of the adsorption isotherm (i.e. the evolution of $\frac{C_e}{Q_e}$ vs C_e) are presented in

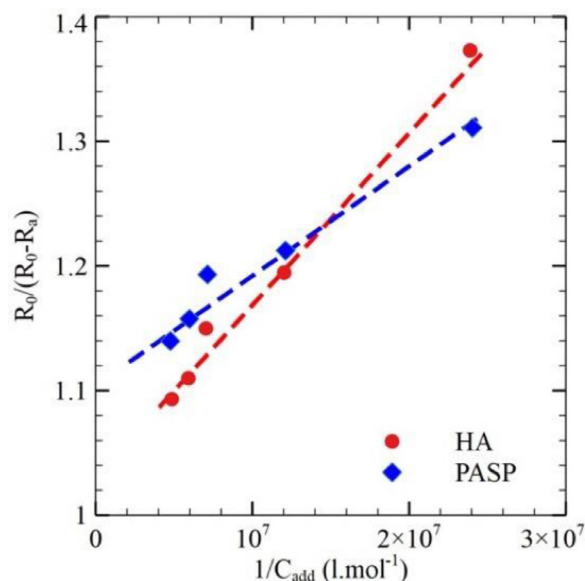


Fig. 7. HA and PASP concentration effects on crystal growth inhibition. $\Omega = 7.6$, at 35°C and $100 \text{ mg}\cdot\text{L}^{-1}$ calcite seeds.

Table 5

Adsorption characteristics at 35°C , with $100 \text{ mg}\cdot\text{L}^{-1}$ calcite seeds and 7.6 supersaturation ratio.

Adsorption characteristics	HA	PASP
$(1 - b)$	0.971	0.900
$K_a (\text{L}\cdot\text{mol}^{-1})$	5.0×10^7	1.0×10^8

Supplementary Material Fig. SM4. In the case of experiments performed with HA polymer, the correct fit confirms that the main mechanism of crystal growth inhibition is due to adsorption of the polymer on the surface of calcite crystals.

When PASP is added to the solution, the obtained result is less clear. The hypothesis of adsorption mechanism seems to be valid to a concentration up to $5 \text{ mg}\cdot\text{L}^{-1}$. But, for higher concentrations, a deviation from linearity is observed that could be due to an adsorption mechanism that is not described by the Langmuir model,

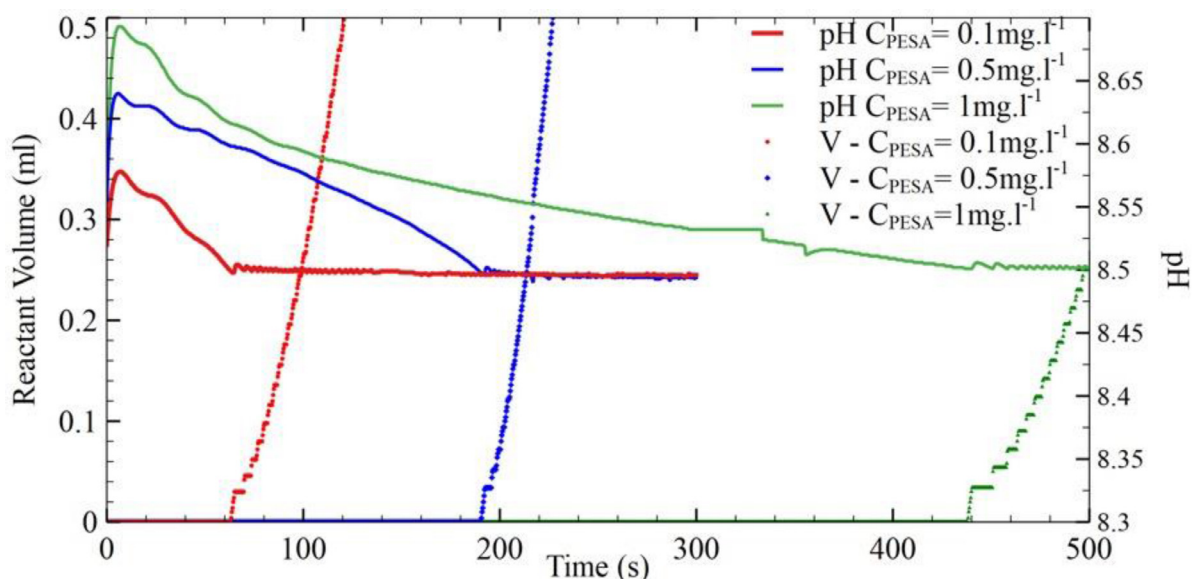


Fig. 6. Temporal evolution of pH and added reagent volume during constant composition experiments performed at $T=35^\circ\text{C}$ and $\Omega=7.6$ with concentrations of PESA ranging from 0.1 to $1 \text{ mg}\cdot\text{L}^{-1}$.

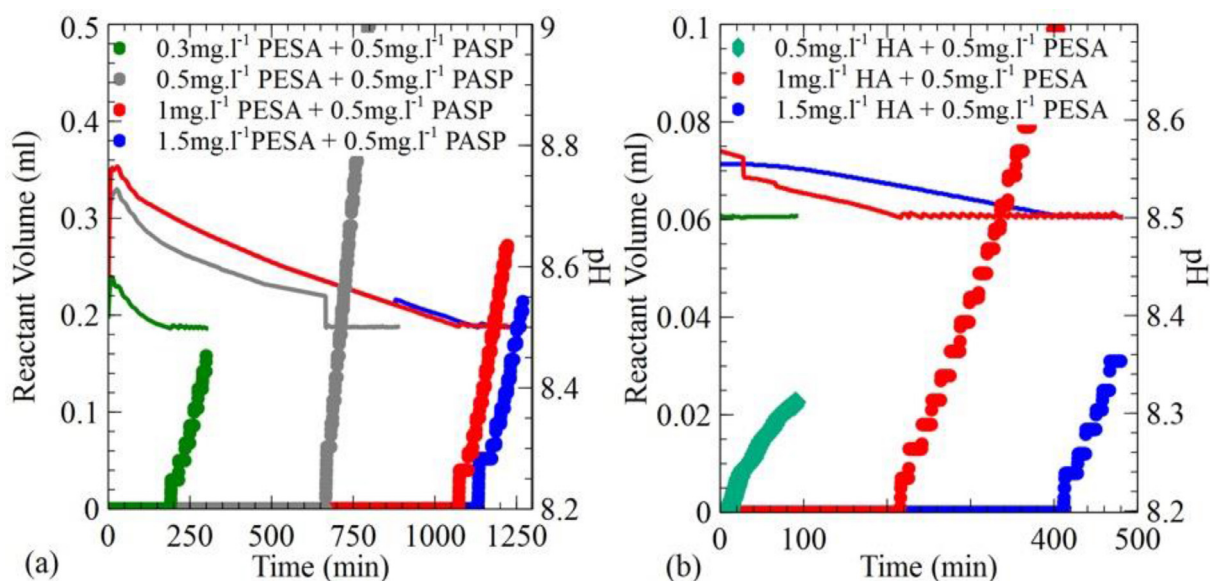


Fig. 8. Temporal evolution of pH and added reagent volume during constant composition experiments performed at $T=35^{\circ}\text{C}$ and $\Omega=7.6$ with different mixtures of (a) PESA and PASP (b) PESA and HA.

Table 6

Adsorption characteristics on adsorption bench test in a solution with 7.6 supersaturation at 35°C in presence of calcite seeds at $100\text{ mg}\cdot\text{L}^{-1}$.

Adsorption characteristics	HA	PASP
Q_m ($\text{mol}\cdot\text{g}^{-1}\text{seeds}$)	2.5×10^{-6}	10^{-6}
K_a ($\text{L}\cdot\text{mol}^{-1}$)	2.3×10^7	1.1×10^8

or by another phenomenon that consume the polymer in solution. In these experiments, the adsorption constants are obtained from the linearized Langmuir model and are given in Table 6.

So, the value of the adsorption affinity constant (K_a) obtained by two different types of experiments (constant composition method and adsorption measurement) are of the same order of magnitude.

3.5. Effect of mixing PASP and PESA or HA and PESA

It is therefore deemed interesting to study the effect of mixtures of growth and nucleation inhibitor additives, under the same experimental conditions: i.e., $\Omega = 7.6$, temperature 35°C , calcite seeds at $100\text{ mg}\cdot\text{L}^{-1}$. Two series of tests were carried out: PASP+PESA and HA+PESA. Growth inhibitor (HA or PASP) concentration was held constant at $0.5\text{ mg}\cdot\text{L}^{-1}$ while nucleation inhibitor concentration was varied between 0.3 and $1.5\text{ mg}\cdot\text{L}^{-1}$. The performance indicators of scale inhibition were the delay time of crystallization and the inhibition rate.

Fig. 8A shows the evolution of reagent volume addition during the experiments at constant composition for PESA+PASP mixtures and Table 7 shows the values of the delay time of crystallization and inhibition rate for various concentrations of PESA in the PESA+PASP mixture.

In the case of PESA and PASP mixtures (Fig. 8A), the results show that a positive synergetic effect is obtained on delay time when additives are mixed. For instance, for the experiment performed with $0.5\text{ mg}\cdot\text{L}^{-1}$ of PESA in the mixture, a delay time of 666 min is measured whereas it is of 190 min with the same concentration of PESA used alone. In addition, this experiment was performed with a total additive concentration of $1\text{ mg}\cdot\text{L}^{-1}$, and can be compared with experiment performed with PESA alone at the

same concentration with a lower delay time for crystallization (i.e. 438 min).

Apparent delay time increased with increasing PESA concentration in the mixture. In addition, as PESA concentration in the mixture was increased from $1\text{ mg}\cdot\text{L}^{-1}$ to $1.5\text{ mg}\cdot\text{L}^{-1}$, apparent delay increased from 1,072.3 minutes to 1,128.6 minutes (Fig. 8A), which is more than twice the delay time obtained when PESA is not mixed with PASP. After the delay time of crystallization, crystallization starts with approximately the same rate as the one obtained with PASP used alone. The inhibition rate is 87% for PASP alone and ranges between 85% to 89% when PASP is used in a mixture with PESA.

Fig. 8B shows the evolution of reagent volume addition during the experiments at constant composition for the PESA+HA mixtures and Table 8 shows the values of the delay time of crystallization, the growth rate and the inhibition rate for various concentrations of PESA in the PESA+HA mixtures. The results obtained show that no synergetic effect is obtained when both additives are mixed. The result obtained is a combination of both effects: PESA addition increases the delay time of crystallization whereas HA addition decreases the crystal growth rate. The experiment performed with $0.5\text{ mg}\cdot\text{L}^{-1}$ of PESA (corresponding to a total concentration of additives of $1\text{ mg}\cdot\text{L}^{-1}$) in the mixture have a much lower delay time for crystallization than the one obtained for PESA alone. In addition, under the same conditions as for the PESA + PASP mixture, apparent delay time was much shorter with PESA + HA (Table 8). The inhibition rate of crystal growth is slightly increased (from 92% to 97%) by the presence of PESA when compared to the experiment performed with HA alone.

Fig. 9 shows SEM images of crystals grown with various PESA and PASP mixtures. The mixture showed predominance of calcite and vaterite crystals, whatever the concentration of PESA.

4. Discussion

The results obtained in this study, raise three important questions. Why vaterite is mainly formed when PASP is added to the supersaturated solution even in presence of stable calcite? Why such crystallization delay time is obtained in presence of PESA? Why only PESA and PASP mixture shows a significant synergetic effect?

Table 7

Effect of PESA concentration in a PESA+PASP mix on various performance indicators, at 7.6 supersaturation at 35°C in presence of calcite seeds at 100 mg·L⁻¹.

PESA + PASP mix	Apparent delay time (min)	R _a (mol·m ⁻² ·min ⁻¹)	Inhibition rate (%)
PESA 0.3 + PASP 0.5	191.0	6.39×10^{-6}	89.5
PESA 0.5 + PASP 0.5	665.6	7.98×10^{-6}	86.9
PESA 1.0 + PASP 0.5	1072.3	9.05×10^{-6}	85.1
PESA 1.5 + PASP 0.5	1128.6	6.92×10^{-6}	88.6

Table 8

Effect of PESA concentration in a PESA+HA mix on various performance indicators, at 7.6 supersaturation at 35°C in presence of calcite seeds at 100 mg·L⁻¹.

PESA + HA mix	Apparent delay time (min)	R _a (mol·m ⁻² ·min ⁻¹)	Inhibition rate (%)
PESA 0.5 + HA 0.5	11.0	1.60×10^{-6}	97.4
PESA 1.0 + HA 0.5	216.3	2.66×10^{-6}	95.6
PESA 1.5 + HA 0.5	411.0	2.13×10^{-6}	96.5

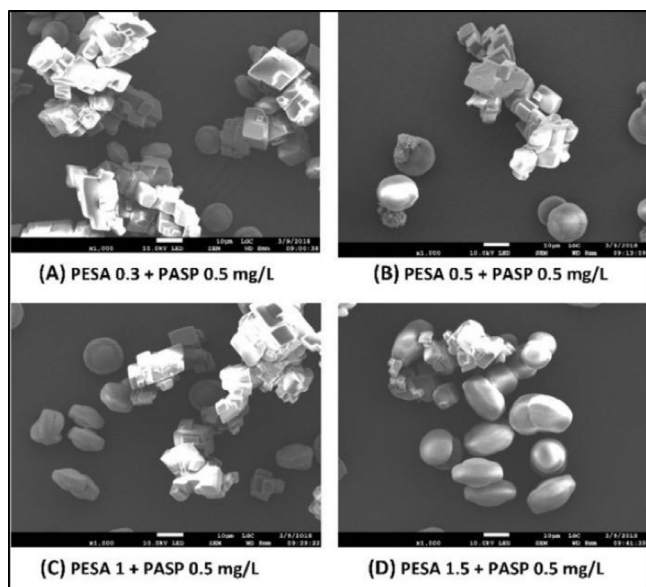


Fig. 9. SEM images for mixtures of various PESA concentrations with PASP at 0.5 mg·L⁻¹.

When HA is added to the growing medium, no crystallization delay is observed, but crystal growth is strongly slowed down. Based on adsorption experiments and simulations results found in literature (Tribello et al., 2009; Bulo et al., 2007) it is more likely that crystal growth inhibition is mainly due to adsorption of the polymer on the crystal surface rather than binding of the acrylate polymer to Ca²⁺ ion / carbonate ions in solution. Moreover, because of the very low concentration of additive and due to the use of the constant composition set-up (presence of calcite seeds), no effect on nucleation was observed at the opposite of the study of Gebauer et al. (2009). In these conditions, HA inhibitor can be referenced as a crystal growth inhibitor by adsorption on crystal faces (type IV of the Gebauer et al., 2009 classification: “the additive adsorbs onto the nucleated particles and stabilizes them”).

The influence of PASP on calcium carbonate crystallization is subtler to analyze. The results of constant composition crystal growth experiments show that with the addition of PASP, a slight increase of delay time is observed and crystal growth on calcite seeds is also strongly slowed down. Adsorption experiments show that the adsorption of PASP on crystal surfaces is less effective, and a change on the adsorption isotherm is observed beyond a certain concentration. In addition, the introduction of PASP in the

growing medium, moves the crystallization of calcium carbonate towards the crystallization of vaterite, even in presence of calcite. As proposed by Grower and Odom (2000), it is clear that the adsorption of polymer on crystal surface cannot provide a full explanation of the PASP additive action on crystal morphology. As presented in Fig. 4(B), the crystallization pumpkin particles and the “double-leaf” type of particles suggest that, based on the work of Xu et al. (2014), the main crystallization mechanism proceeds via the formation of an amorphous calcium carbonate (ACC) phase. Compared to the reference experiments (without additives) or experiments performed in presence of HA, the orientation of crystallization of calcium carbonate towards a metastable phase with PASP (i.e. vaterite) suggests that one of the main effects of PASP is to control the local structure of the nucleated secondary phase (type VI of additives in the Gebauer’s classification). Consequently, PASP inhibits the formation of calcite. A possible mechanism of crystal inhibition due to the presence of PASP, could be that this additive promotes the formation of a Polymer Induced Liquid Phase (PILP). Indeed, as the concentration of polymer is low, this liquid phase could not be stabilized and was quickly transformed in ACC, as suggested in some conditions by Gebauer et al.(2009) and Grower and Odom (2000). Then, this ACC turns into vaterite.

Unlike to the other two polymers, PESA acts differently: no inhibition of crystal growth but strong inhibition of nucleation (see Fig. 8) is obtained. In addition, as for HA, XRD and SEM analyzes show that only calcite crystals are obtained. As pointed out by Pesonen et al.(2005), PESA is a very efficient chelator leading to a decrease of available Ca²⁺ ions in solution and thus to a decrease of supersaturation. This could explain the inhibition of nucleation. Moreover, the simulation of Pesonen et al.(2005) showed that the formed complexes are very stable.

However, this chelation effect does not explain the fact that when crystallization starts after the delay time, the consumption of reagent is of the same order of magnitude or higher than the one obtained without additives (higher growth rate). To explain this behavior, complementary free Ca²⁺ titration experiments were performed, (see Fig. SM5 in Supplementary Material). These experiments were performed at 35°C at constant polymer concentration (0.5 mg·L⁻¹) and different supersaturation ratio (from 7.6 to 12). The results show that whatever the supersaturation ratio, the free Ca²⁺ concentration drops always to the same value around 8.310^{-3} mol/L⁻¹ and remains stable until the beginning of the crystallization. It is also important to notice that the crystallization delay time depends either on supersaturation either on polymer concentration. The corresponding ion activity product ($\log IAP = a_{Ca^{2+}} a_{CO_3^{2-}} = -7.56$) is closed to the solubility product of ACC phases (I and II) calculated by Gebauer et al.(2009) $\log k_{ACC_i} =$

-7.51 and $\log k_{ACC_{II}} = -7.42$. This result suggests that the addition of PESA induces the precipitation of an amorphous phase (for which we cannot state whether it is LIPS or solid) and this polymer stabilizes this metastable intermediate phase, precursor of calcite crystals. The formation of calcite is then either due to an abrupt transformation of ACC to calcite (secondary nucleation) either to deposition/aggregation of this amorphous ACC on the existing surface calcite seeds which explain the roughness of the observed crystals.

The three additives tested in this study (HA, PASP and PESA) show three different action ways, that explain the synergetic effects found when two additives are mixed. For instance, mixing an inhibitor of crystal nucleation (PESA) and a crystal growth inhibitor (HA) allows to delay crystal nucleation (with the action of PESA), but also to decrease crystal growth rate, thanks to the adsorption of HA on the surface the newly formed crystals on the seeds. However, the synergetic effect of mixing these two additives is not as efficient as it can be expected. Indeed, even if the crystal growth rate (or the flow rate of reagent addition) is close to the one obtained with HA alone, the delay time observed in the case of the mixture (PESA + HA) is much lower than the one obtained with PESA alone. This could be due to molecular interaction or oligomerization between the two polyelectrolytes in solution that decreases the amount of free groups available for Ca^{2+} complexation (smaller increase of pH at the beginning of the experiments compared to PESA alone). Surprisingly, the reverse is observed when PASP and PESA are mixed: even if the inhibition rate is almost the same (than in the previous case), the delay time of crystallization is at least twice the one obtained with PESA alone. By taking the assumption that the presence of PASP cancels the formation route of calcite (and thus promotes the formation of vaterite), then the ACC stabilized by the presence of PESA, cannot turn into calcite, which delays crystallization.

From a practical point of view, using a mixture of PESA and PASP provides a promising approach for scale inhibition. Under the experimental conditions applied in this study, maximum apparent delay time was nearly 19 hours, with inhibition rate close to 89% for a mixture of PESA at $1.5 \text{ mg}\cdot\text{L}^{-1}$ and PASP at $0.5 \text{ mg}\cdot\text{L}^{-1}$. In comparison, mean residence time in industrial cooling circuits is around 24 hours; thus, a PESA-PASP mixture (both green additives) should significantly reduce scaling by acting on nucleation and crystal growth. In addition, the formation of aggregated vaterite particles with pumpkins shape make the deposit more porous and thus less adherent to the surface.

5. Conclusion

The scaling inhibition efficacy of three polymer additives, HA, PASP and PESA, was assessed under conditions representative of industrial cooling circuits using a constant composition method developed in our previous research. Technically, this approach allows to study, close to industrial conditions (water hardness, temperature, suspended matter...) the scaling behavior of real water. From a practical point of view, by understanding and measuring the influence of each additive alone on the crystallization of calcium carbonate, this approach has enabled to design efficient mixture of additives to avoid or delay scale formation. We have shown that by mixing two additives showing two different acting ways, it is possible either to combine their effects or to improve their inhibitory effect. For instance, nearly 19 hours, with inhibition rate close to 89% was found for a mixture of PESA and PASP even for a solution with relatively high supersaturation ratio and containing seeds of calcite. These findings open highly promising perspectives for preventive scaling treatment, improving the thermal efficacy of heat exchangers in industrial cooling circuits.

Declaration of Competing Interest

The authors declare that they have no known competing financial interests or personal relationships that could have appeared to influence the work reported in this paper.

Acknowledgments

The authors wish to thank Marie-Line de Solan-Bethmale from the Laboratoire de Génie Chimique (LGC) for the SEM analyses and Cédric Charvillat from the Centre Interuniversitaire de Recherche et d'Ingénierie des Matériaux (CIRIMAT) for the powder XRD measurements.

Supplementary materials

Supplementary material associated with this article can be found, in the online version, at [doi:10.1016/j.watres.2020.116334](https://doi.org/10.1016/j.watres.2020.116334).

Appendix: Adsorption bench test and experimental conditions

Three models are widely used for isotherms: Langmuir, Freundlich and Redlich-Peterson (Liu et al., 2010). For calcium carbonate crystal growth inhibition by polymer additives, the Langmuir model is the most widely used to describe additive molecule adsorption on growth site surfaces (Dimova et al., 2003; Dalas et al., 2006; Zhang et al., 2016; Lisitsin et al., 2009; Klepetsanis et al., 2002).

The model is based on 3 assumptions:

- The adsorbent exposes a limited number of adsorption sites: i.e., has a maximum adsorption capacity, Q_m .
- All adsorption sites are identical and receive only 1 molecule at a time.
- At binding, the energy between site and adsorbed molecule is constant, unaffected by adsorption at neighboring sites.

Under controlled temperature, adsorption isotherms depend on the type of adsorbent (calcite seeds or suspended matter) and on the type of adsorbed molecules (polymer additive molecules). This dependence is represented by an equation relating quantity of adsorbed polymer (Q_e) to additive molecules equilibrium concentration (Liu et al., 2010; Blachier et al., 2009).

$$Q_e = \frac{V(C_{\text{add}} - C_e)}{m} \quad (\text{A1})$$

where Q_e is the quantity of polymer adsorbed by the adsorbent ($\text{mol}\cdot\text{g}^{-1}$), V is the solution volume (L), C_{add} and C_e are respectively the initial and the residual post-equilibrium polymer concentration ($\text{mol}\cdot\text{L}^{-1}$), and m is the adsorbent (seeds) mass (g).

The Langmuir adsorption isotherm model is a representation of $Q_e = f(C_e)$ with the following non-linear expression:

$$Q_e = Q_m \frac{K_a C_e}{1 + K_a C_e} \quad (\text{A2})$$

where Q_m is the maximum adsorption capacity (in mole polymer per g calcite seeds), and K_a is the Langmuir adsorption affinity constant ($\text{L}\cdot\text{mol}^{-1}$).

Constants Q_m and K_a can be determined experimentally by linearizing relation (2) as $\frac{C_e}{Q_e} = \frac{1}{Q_m} C_e + \frac{1}{Q_m K_a}$ and tracing $\frac{C_e}{Q_e} = f(C_e)$.

To consolidate the adsorption characteristics obtained on the constant composition set-up, an adsorption test bench was implemented (Fig. A1).

The test bench comprised:

- a thermostatic bath at 35°C in which a magnetic stir table is immersed;

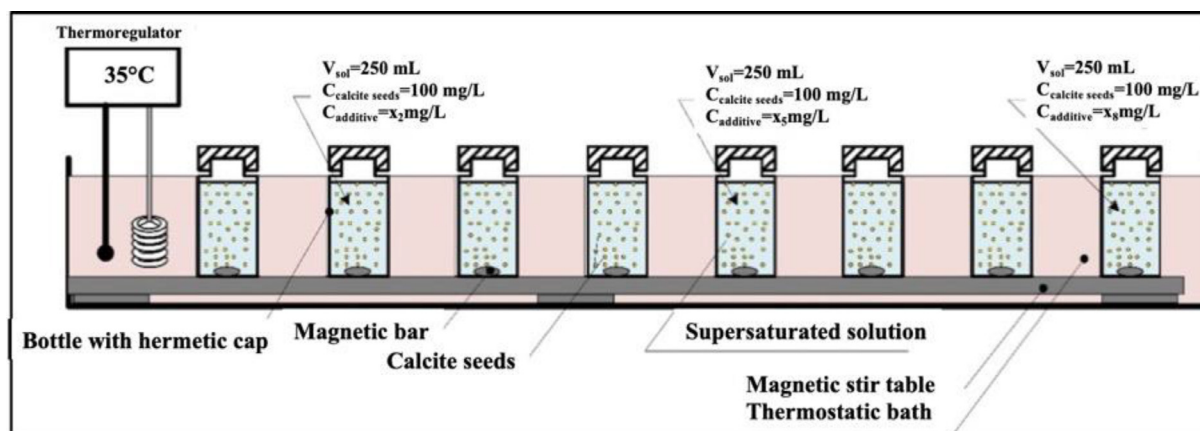


Fig. A1. Adsorption test bench for polymer additive molecules in solution at constant supersaturation in presence of calcite seeds at constant concentration.

- a series of 8 identical hermetically capped bottles with identical magnetic bars;
- each bottle is filed with 200 mL solution at 7.6 supersaturation;
- solution temperature is held at 35°C;
- in each bottle, a constant mass of calcite seed (20 mg) is introduced, for a concentration of 100 mg·L⁻¹;
- at $t = 0$, the test additive is added at concentrations from 0.1 to 1.2 mg·L⁻¹, a range set by the assay limit of quantification for residual additive at end of test;
- after 6 days' contact, the solutions are filtered at 0.2 μm , collecting filtrate for assay of residual additive and of calcite seed for SEM characterization.

Residual additive concentration (C_e) in the solution at 7.6 supersaturation at end of each test was assayed on UV-Visible spectrophotometry using 2 reagents: benzethonium chloride and trisodium citrate dihydrate. The assay principle is based on proportionality between turbidity and additive concentration. Turbidity is caused by the reaction between benzethonium chloride and the functional groups of the polymer additive. Trisodium citrate dihydrate is needed to complex the free calcium ions in the sample in order to reduce interference resulting from complexation by polymer additive molecules. All assays were performed on a double-beam Shimadzu 1800 spectrophotometer with 10 cm quartz optical trajectory tanks, with working wavelength set at 306 nm. This tank length reduces the limit of quantification to 0.1 mg·L⁻¹, enabling assay of low polymer additive concentrations after the adsorption tests.

References

Al-Hamzah, A.A., East, C.P., Doherty, W.O.S., Fellows, C.M., 2014. Inhibition of homogenous formation of calcium carbonate by poly(acrylic acid). The effect of molar mass and end-group functionality. *Desalination* 338, 93–105.

Al-Hamzah, A.A., Fellows, C.M., 2015. A comparative study of novel scale inhibitors with commercial scale inhibitors used in seawater desalination. *Desalination* 359, 22–25.

Al-Rawajfeh, A., 2008. Simultaneous desorption-crystallization of CO₂-CaCO₃ in multistage flash (MSF) distillers. *Chem. Eng. Process.* 47, 2262–2269.

Amjad, Z., Landgraf, R.T., Penn, J.L., 2014. Calcium sulfate dihydrate (gypsum) scale inhibition by PAA, PAPEMP, and PAA/PAPEMP blend. *Int. J. Corros. Scale Inhib.* 3, 35–47.

Blachier, C., Michot, L., Bihannic, I., Barrès, O., Jacquet, A., Mosquet, M., 2009. Adsorption of polyamine on clay minerals. *J. Colloid Interface Sci.* 336, 599–606.

Bu, Y., Zhou, Y., Yao, Q., Chen, Y., Sun, W., Wu, W., 2016. Inhibition of calcium carbonate and sulfate scales by a non-phosphorus terpolymer AA-APEY-AMPS. *Desalin. Water Treat.* 57, 1977–1987.

Bulo, R. E., Donadio, D., Laio, A., Molnar, F., Rieger, J., Parrinello, M., 2007. Site binding of Ca²⁺ ions to polyacrylates in water: a molecular dynamics study of coiling and aggregation. *Macromolecules* 40, 3437–3442.

Chaussemier, M., Pourmohtasham, E., Gelus, D., Pécou, N., Perrot, H., Lédion, J., Charpentier, H.C., Horner, O., 2015. State of art of natural inhibitors of calcium. A review article. *Desalination* 356, 47–55.

Cheap-Charpentier, H., Horner, O., Lédion, J., Perrot, H., 2018. Study of the influence of the supersaturation coefficient on scaling rate using the pre-calcified surface of a quartz crystal microbalance. *Water Res.* 142, 347–353. IWA Publishing, 2018.

Chhim, N., Kharbachi, C., Neveux, T., Bouteleux, C., Teychené, S., Biscans, B., 2017. Inhibition of calcium carbonate crystal growth by organic additives using the constant composition method in conditions of recirculating cooling circuits. *J. Cryst. Growth* 472, 35–45.

Dalas, E., Chalias, A., Gatos, D., Barlos, K., 2006. The inhibition of calcium carbonate crystal growth by the cysteine-rich Mdm2 peptide. *J. Colloid Interface Sci.* 300, 536–542.

Dimova, R., Lipowsky, R., Mastai, Y., Antonietti, M., 2003. Binding of polymers to calcite crystals in water: characterization by isothermal titration calorimetry. *Langmuir* 19, 6097–6103.

Gebauer, D., Colfen, H., Verch, A., Antonietti, M., 2009. The multiple roles of additives in CaCO₃ crystallization: a quantitative case study. *Adv. Mater.* 21 (Issue 4), 435–439. doi:10.1002/adma.200801614.

Ghani, S., Al-Defferi, N.S., 2010. Impacts of different antiscalant dosing rates and their thermal performance in Multi Stage Flash (MSF) distiller in Kuwait. *Desalination* 250, 463–472.

Girasa, W., De Wispelaere, M., 2004. Polyaspartate, an new alternative for the conditioning of cooling water. 14th International Conference on the Properties of Water and Steam Aug 29–Sep 3.

Grower, L.B., Odom, D.J., 2000. Deposition of calcium carbonate films by a polymer-induced liquid-precursor (PILP) process. *J. Cryst. Growth* 210 (issue 4), 719–734. doi:10.1016/S0022-0248(99)00749-6.

Harris, K., 2011. Biodegradation and testing of scale inhibitors. *Chem. Eng.* 49–53.

Hasson, D., Shemer, H., Sher, A., 2011. State of the art of friendly “Green” scale control inhibitors: a review article. *Ind. Eng. Chem. Res.* 50, 7601–7607.

Heming, L., Dejun, C., Xiaoping, Y., 2015. Synthesis and performance of a polymeric scale inhibitor for oilfield application. *J. Petrol. Explor. Prod. Technol.* 5, 177–187.

Idlaflkih, Z., Cossa, D., Meybeck, M., 1995. Comportements des contaminants en trace dissous et particulaires (As, Cd, Cu, Hg, Pb, Zn) dans la Seine. *Hydroécol. Appl.* 127–150. doi:10.1051/hydro:1995008.

Kirboga, S., Oner, M., 2012. The inhibitory effects of carboxymethyl inulin on the seeded growth of calcium carbonate. *Colloids Surf. B* 91, 18–25.

Klepetsanis, P.G., Koutsoukos, P.G., Chitanu, G-C., Carпов, A., 2002. The inhibition of calcium carbonate formation by copolymers containing maleic acid. In: Amjad, Z. (Ed.), *Water Soluble Polymers*. Plenum Press, New York, pp. 117–129.

Lioliou, M.G., Paraskeva, C.A., Koutsoukos, P.G., Payatakes, A.C., 2006. Calcium sulfate precipitation in presence of water-soluble polymers. *J. Colloid Interface Sci.* 303, 164–170.

Litsin, D., Hasson, D., Semiat, R., 2009. Modeling the effect of anti-scalant on CaCO₃ precipitation in continuous flow. *Desalin. Water Treat.* 1, 17–24.

Liu, D., Dong, W., Li, F., Hui, F., Lédion, J., 2012. Comparative performance of polyepoxysuccinic acid and polyaspartic acid on scaling inhibition by static and rapid controlled precipitation methods. *Desalination* 304, 1–10.

Liu, Q-S., Zheng, T., Wan, P., Jiang, J-P., Li, N., 2010. Adsorption isotherm, kinetic and mechanism studies of some substituted phenols on activated carbon fibers. *Chem. Eng. J.* 157 (2–3), 348–356.

Martinod, A., Neville, A., Euvrad, M., Sorbie, K., 2009. Electrodeposition of a calcareous layer: effects of green inhibitors. *Chem. Eng. Sci.* 64, 2413–2421.

Moulaya, S., Boukherissa, M., Abdoune, F., Benabdelmoumene, F.Z., 2005. Low molecular weight poly(acrylic acid) as a Salt scaling inhibitor in oilfield operations. *J. Iran. Chem. Soc.* 2, 212–219.

Neveux, T., Bretaude, M., Chhim, N., Shakourzadeh, K., Rapenne, S., 2016. Pilot plant experiments and modeling of CaCO₃ growth inhibition by the use of antiscalant polymers in recirculating cooling circuits. *Desalination* 397, 43–52.

Parsiegla, K.I., Katz, J.L., 1999. Calcite growth inhibition by copper (II) I. Effect of supersaturation. *J. Cryst. Growth* 200, 213–226.

- Peronno, D., Cheap-Charpentier, H., Horner, O., Perrot, H., 2015. Study of the inhibition effect of two polymers on calcium carbonate formation by fast controlled precipitation method and quartz crystal microbalance. *J. Water Process Eng.* 7, 11–20.
- Pesonen, H., Sillanpää, A.J., Laasonen, K., 2005. Density functional complexation study of metal ions with poly(carboxylic acid) ligands. Part 2. Poly(acrylic acid-co-maleic acid), poly(methyl vinyl ether-co-maleic acid), and poly(epoxy succinic acid). *Polymer* 46 (26), 12653–12661.
- Phuntsho, S., Lotfi, F., Hong, S., Shaffer, D.L., Elimelech, M., Shon, H.K., 2014. Membrane scaling and flux decline during fertiliser-drawn forward osmosis desalination of brackish. *Water Res.* 57, 172–182.
- Pramanik, B.K., Gao, Y., Fan, L., Roddick, F.A., Liu, Z., 2017. Antiscaling effect of polyaspartic acid and its derivative for RO membranes used for saline wastewater and brackish water desalination. *Desalination* 404, 224–229.
- Quan, ZH., Chen, YC., Wang, XR., Shi, C., Liu, YJ., Ma, CF., 2008. Experimental study on scale inhibition performance of a green scale inhibitor polyaspartic acid. *Sci. China Ser. B-Chem.* 51 (7), 695–699.
- Rahmani, Kh., Jadidian, R., Haghtalab, S., 2015. Evaluation of inhibitors and biocides on the corrosion, scaling and biofouling control of carbon steel and copper-nickel alloys in a power plant cooling water system. *Desalination* 393, 174–185.
- Rodriguez Blanco, J.D., Shaw, S., Benning, L.G., 2011. The kinetics and mechanisms of amorphous calcium carbonate (ACC) crystallization to calcite, via vaterite. *Nanoscale* 3, 265.
- Schweinsberg, M., Hater, W., Verdes, J., 2003. New stable biodegradable scale inhibitor formulations for cooling water: development and field tests. 64th International Water Conference Oct 19–23.
- Shen, Z., Li, J., Xu, K., Ding, L., Ren, H., 2012. The effect of synthesized hydrolyzed polymaleic anhydride (HPMA) on the crystal of calcium carbonate. *Desalination* 284, 238–244.
- Sun, Y.H., Xiang, W.H., Wang, Y., 2009. Study on polyepoxysuccinic acid reverse osmosis scale inhibitor. *J. Environ. Sci.* 21, 73–75.
- Tribello, G.A., Bruneval, F., Liew, C.C., Parrinello, M., 2009. A molecular dynamics study of the early stages of calcium carbonate growth. *J. Phys. Chem. B* 113 (34), 11680–11687.
- Wilson, D.K., Harris, K.M., 2011. Development of a 'Green' hydrothermally stable scale inhibitor for geothermal wells and pipelines. In: *Proceedings International Workshop on Mineral Scaling*, pp. 107–112.
- Xu, Y., Guobin, M., Wang, M., 2014. Fabrication and growth mechanism of pumpkin-shaped vaterite hierarchical structures. *Cryst. Growth Des.* 14 (12), 6166–6171. <https://doi.org/10.1021/cg501477u>.
- Zhang, S., Sheng, J.J., Qiu, Z., 2016. Water adsorption on kaolinite and illite after polyamine adsorption. *J. Petroleum Sci. Eng.* 142, 13–20.
- Zhou, X., Sun, Y., Wang, Y., 2011. Inhibition and dispersion of polyepoxysuccinate as a scale inhibitor. *J. Environ. Sci.* 23, 159–161.